Measurements of contrast sensitivity for peripheral vision

Michał Chwesiuk
West Pomeranian University of Technology, Szczecin
michalchwesiuk@gmail.com

Radosław Mantiuk
West Pomeranian University of Technology, Szczecin
rmantiuk@zut.edu.pl

ABSTRACT

Contrast detection thresholds were measured for the eccentricities from 0° to 27° and a range of stimuli frequencies from 0.125*cpd* to 16*cpd*. The measurements were motivated by the need to collect visual performance data for the gaze-contingent rendering system. For this application, the mixed chromatic and achromatic stimuli are even more important than purely chromatic cases. Therefore, the detection of sine-gratings with Gaussian patches was measured for four mixed chromatic/achromatic with a varying share of the achromatic components. To verify that our experimental setup generates the results consistent with the previous work, we also measured the contrast thresholds for achromatic (black to white) stimulus. Five observers participated in the experiments and they individually determined the detection threshold for each stimulus using the QUEST method. The results plotted as the contrast sensitivity function (CSF) follow the state-of-the-art CSF models. However, we report lower sensitivity to contrast for achromatic stimuli caused by the small size of the stimulus. The color directions closer to the chromatic green-to-red axis show higher contrast sensitivity in comparison to achromatic stimuli, while for the yellow-to-blue axis the sensitivity is lower. The higher achromatic component in the mixed stimuli approaches contrast sensitivity to the achromatic CSF.

CCS CONCEPTS

• **Computing methodologies** → **Perception**; **Visibility**.

KEYWORDS

contrast detection thresholds, gaze-dependent contrast thresholds, contrast sensitivity function, gaze-contingent display, gaze-dependent rendering, eye tracking, psychophysical experiments

ACM Reference Format:
Michał Chwesiuk and Radosław Mantiuk. 2019. Measurements of contrast sensitivity for peripheral vision. In *ACM Symposium on Applied Perception 2019 (SAP '19), September 19–20, 2019, Barcelona, Spain.* ACM, New York, NY, USA, 9 pages. https://doi.org/10.1145/3343036.3343123

Permission to make digital or hard copies of all or part of this work for personal or classroom use is granted without fee provided that copies are not made or distributed for profit or commercial advantage and that copies bear this notice and the full citation on the first page. Copyrights for components of this work owned by others than ACM must be honored. Abstracting with credit is permitted. To copy otherwise, or republish, to post on servers or to redistribute to lists, requires prior specific permission and/or a fee. Request permissions from permissions@acm.org.
SAP '19, September 19–20, 2019, Barcelona, Spain
© 2019 Association for Computing Machinery.
ACM ISBN 978-1-4503-6890-2/19/09…$15.00
https://doi.org/10.1145/3343036.3343123

1 INTRODUCTION

The *contrast sensitivity function* (CSF) expresses the sensitivity of the human visual system (HVS) to contrast, i.e. ability to detect a pattern in the low contrast conditions. The contrast sensitivity can be measured for a range of frequencies of the pattern as well as for a range of eccentricities. The *contrast thresholds*, i.e. the inverse of contrast sensitivity, are significantly lower in the fovea (for central vision) and quickly increases for the parafoveal and peripheral visions. It varies depending on change in the color of the stimulus, as well as, is different for achromatic, chromatic and mixed chromatic/achromatic color stimuli.

In this study, we measure the contrast sensitivity for two chromatic (green-to-red and yellow-to-blue) and four mixed color directions (pink to green-cyan, green to light-pink, dark-red to cyan, green-yellow to blue-violet). The motivation behind using these very color directions is to test the colors corresponding to the RGB color primaries used in computer graphics applications. The measurement is performed for a range of eccentricities from 0° to 27°. For achromatic stimuli, we measure stimuli of the frequencies from 0.125*cpd* to 16*cpd*. For chromatic and mixed color directions, only frequency of 2*cpd* is tested, for which the achromatic stimuli show the highest sensitivity to contrast.

We perform experiments, in which five observers individually determine the detection threshold for each stimuli using the QUEST adaptive procedure. The results plotted as the contrast sensitivity function follow the state-of-the-art CSF models. The color directions closer to the chromatic green-to-red axis show higher contrast sensitivity in comparison to achromatic stimuli, while for the yellow-to-blue axis the sensitivity is lower. The higher achromatic share in the mixed stimuli approaches contrast sensitivity to the achromatic CSF.

The rest of the paper is organized as follows: in Sect. 2 we discuss previous work on the peripheral contrast threshold measurements, in Sect. 3 the experiment design is explained, the results are reported in Sect. 4.

2 PREVIOUS WORK

The achromatic and chromatic contrast sensitivity functions (CSF) have been measured in a number of studies. Especially, there is extensive literature on measurements for the foveal vision [Mullen 1985; Pelli and Bex 2013; Watson 2000; Wuerger et al. 2002] with an excellent survey presented by Barten [Barten 1999]. Recently, Kim et al. [Kim et al. 2013] measured the contrast thresholds for a wide range of background luminance ranging from 0.02 to 200$cd/m2$, stimuli frequencies from 0.125 to 16*cpd* and the color directions the same as in the ColorFest paper [Wuerger et al. 2002]. We compare our results with their studies in Sect. 4.

Measurements of the peripheral contrast detection involve using a flashing stimuli, which is shown to observer for a short time in the order of tens or hundreds of milliseconds [Anderson et al. 1991; Banks et al. 1991; Cannon 1985; Hilz and Cavonius 1974; Mullen 1991; Peli et al. 1991; Pointer and Hess 1989; Robson and Graham 1981; Thomas 1987]. This flashing ensures that the observer does not turn her/his eyes toward the stimuli and, in this way, unintentionally capture the foveal rather than the peripheral contrast thresholds. In [Chwesiuk and Mantiuk 2017], an approach has been presented in which an eye tracker is used to control the viewing direction. We use this technique in our measurements because it seems to be more convenient for observers and also controls the gaze direction. We compared both flickering and eye tracking techniques in a pilot experiment with comparable results.

The peripheral contrast detection for achromatic stimuli was measured by Robson and Graham [Robson and Graham 1981]. They used 4, 6, 12, and 24cpd patches of horizontal and vertical gratings. This stimulus was displayed for about 100ms but with the temporal filtering of the contrast value within this period. The distances from the gaze point and stimuli were set to 5cm and 14cm. Cannon [Cannon 1985] used 2°-diameter sine-wave grating patches for spatial frequencies of 2, 4, 8, and 16cpd, at eccentricities from 0° to 40°. Thomas [Thomas 1987] examined the ability to detect a low-contrast grating and to identify its spatial frequency or orientation at eccentricities ranging from 0° to 17.5°. The methodology of our measurements is inspired in particular by Peli et al. [Peli et al. 1991]. They measured the threshold contrast required for discrimination between horizontal and vertical sinusoidal grating patches (Gabor functions). Measurements were taken at the fovea and at eccentricities of 2.5°, 5.1°, 10.3°, and 22.8° for five spatial frequencies of 1, 2, 4, 8, and 16cpd. The background luminance was set to 37.5cd/m^2. The stimulus was presented for 0.5s with an abrupt onset and offset.

There have been attempts to model peripheral sensitivity to contrast for chromatic stimuli, mainly to examine mechanisms of the cone and rod vision separately [Anderson et al. 1991; Boynton and Kambe 1980; Gordon and Abramov 1977; Nagy and Doyal 1993; Nagy and Wolf 1993; Noorlander et al. 1983]. Mullen [Mullen 1991] performed experiments address the question of whether there is evidence that the central visual field is any more specialized for color than it is for luminance contrast detection. The decline in contrast sensitivity across the visual field for color-only (red-green) gratings was compared to that for monochromatic luminance gratings at a range of spatial frequency of 2cpd at the fovea and at eccentricities of 10° and 18°. In [Anderson et al. 1991] CSF were measured for eccentricities from 0° to 55° for chromatic red-green sinusoidal stimuli. They report that chromatic acuity declines more steeply than luminance acuity with eccentricity suggesting that there are additional post-receptoral limitations on a color resolution in the periphery. Newton and Eskew [Newton and Eskew 2003] explored differences in the sensitivity of peripheral color mechanisms with detection and discrimination of 2° spots at 18° eccentricity. Nagy and Wolf [Nagy and Wolf 1993] measured color discrimination thresholds for four colors from the red-green portion of the visible spectrum at three locations on the nasal retina (eccentricities of 5°, 20° and 40°). In [Nagy and Doyal 1993] the red-green color-discrimination thresholds were measured for varying stimuli size at eccentricities of 10° and 25°. Five circular stimuli with diameters of 0.5°, 1°, 2°, 4°, and 8° were used at an eccentricity of 10°. At an eccentricity of 25°, fields with diameters of 1°, 2°, 4°, 8°, and 16° were used. The luminance of all stimuli was held constant at 17$cd/m2$. The achieved results support the view that when peripherally viewed stimulus fields are large, discrimination thresholds are similar to those measured with smaller fields in the fovea. In [Mullen and Kingdom 2002] the cone contrast sensitivities for sine-wave grating stimuli (smoothly enveloped in space and time) were measured for the two color systems (RG & BY) and the achromatic system at a range of eccentricities in the nasal field (0°-25° deg). They found that while red-green cone opponency has a steep decline away from the fovea, the loss in blue-yellow cone opponency is more gradual, showing a similar loss to that found for achromatic vision. Mullen et al. [Mullen et al. 2005] measured the cone contrast for red-greed and blue-yellow color directions. They used as a stimulus a radially modulated sine-wave arc, Gaussian enveloped in both angular and radial directions. They report that red-green cone opponency declines steeply across the human periphery and becomes behaviorally absent by 25°-30°. Hansen et al. [Hansen et al. 2009] captured the chromatic color directions at eccentricities of up to 50°. They found that chromatic detection gets worse with increasing eccentricity but is still possible even at large eccentricities. In [Díez-Ajenjo et al. 2011] the chromatic contrast sensitivity was measured at 21 locations in the visual field (including the fovea). Recently, Vanston and Crognale [Vanston and Crognale 2018] report that despite increasing stimulus size in the periphery, the red-green axis stimuli is still perceived as reduced in contrast, whereas the S axis perceived contrast is observed to increase with eccentricity.

3 EXPERIMENT DESIGN

The goal of the experiment was to measure human binocular sensitivity to contrast for a range of eccentricities, stimulus frequencies and color directions. We use new color directions that includes mixed chromatic and achromatic components.

3.1 Stimuli

The stimuli consisted of sine-gratings attenuated by a Gaussian envelope (see Fig. 2). To render stimuli, we used the *CreateProceduralGabor()* and *Screen('DrawTexture', ...)* functions from the Psychtoolbox Matlab toolbox [1] [Brainard 1997]. Actually, the stimulus was displayed using GPU shaders controlled by a set of parameters defining contrast, frequency, orientation, color, location, and size of the stimulus. The stimulus is drawn using the following function:

$$
\begin{aligned}
F(x, y, ch_{rgb}) &= c \cdot 0.5 \cdot wave(x') \cdot gaussian(x', y') \cdot ch_{rgb} \\
&+ ch_b, \\
wave(x) &= sin(\frac{2\pi}{\lambda} x + \psi), \\
gaussian(x, y) &= exp(-\frac{x^2 + \gamma^2 y^2}{2\sigma^2}), \\
x' &= x \cdot cos(\theta) + y \cdot sin(\theta), \\
y' &= -x \cdot sin(\theta) + y \cdot cos(\theta),
\end{aligned}
$$

[1] http://docs.psychtoolbox.org/CreateProceduralGabor

where (x, y) is a position of the pixel relative to the center of the pattern, $wave(x)$ generates sine-gratings, $gaussian(x, y)$ is a Gaussian envelope, and ch_b is the background color. λ corresponds to inverse of the stimulus frequency, ψ is the phase of the signal (we set it to 90°), σ is the standard deviation of the Gaussian filter used to attenuate the pattern, θ changes orientation to horizontal or vertical, and γ is set to 1 to assure symmetric shape of the Gaussian filter.

The display was calibrated to sRGB color profile with the peak luminance of $120cd/m^2$. ch_{rgb} is a vector of RGB color channel multiplicators. To generate achromatic stimuli, ch_{rgb} was set to $[1, 1, 1]$. For chromatic and mixed chromatic/achromatic stimuli, ch_{rgb} was set to values presented in Tab. 1 (last column). For example for M4 ($ch_{rgb} = [1, 0, 0]$), only the red channel is modulated but as the grey background color is added to all channels, the sine-grating changes from pink to green-cyan.

The background color (ch_b) was set to D65 with the luminance of $48cd/m^2$ (the values measured with the chroma meter were Yxy = [48.37,0.3136,0.3182], LMS = [31.83,16.54,0.45]). The contrasts were selected to avoid luminance levels lower than $1cd/m^2$ and higher than $100cd/m^2$, at which the display calibration was unreliable.

Because of the limitation of the Psychtoolbox *CreateProceduralGabor()* procedure, we used a custom script to draw the chromatic stimuli. The script uses the same model of the sine-grating pattern but ch_b is set to intermediate color between green and red for C2, and between yellow and blue for C3. Additionally, the luminance of the Gaussian envelope was reduced to the luminance of these intermediate colors ($20cd/m^2$ for C2, and $7cd/m^2$ for C3).

All results in the paper are reported in terms of contrast sensitivity S, which is defined as the inverse of the *cone contrast threshold*: $S = 1/C_c$. We use the cone contrast definition used for the ColorFest [Wuerger et al. 2002] study:

$$C_c = \frac{1}{\sqrt{3}}\sqrt{\left(\frac{\Delta L}{L_b}\right)^2 + \left(\frac{\Delta M}{M_b}\right)^2 + \left(\frac{\Delta S}{S_b}\right)^2}, \quad (1)$$

where L_b, M_b, S_b are the LMS trichromatic color values of the background color, and $\Delta L, \Delta M, \Delta S$ are magnitudes of the modulations of the grating. For achromatic stimuli, the definition of the cone contrast simplifies to relative modulation of the sine-grating: $C = (I_{max} - I_{min})/I_b$, where I_b is the background luminance, I_{max} and I_{min} correspond to maximum and minimum luminance of the sine-grating, respectively. After [Kim et al. 2013] we used the following operation:

$$\begin{bmatrix} L \\ M \\ S \end{bmatrix} = \begin{bmatrix} 0.15514 & 0.54312 & -0.03286 \\ -0.15514 & 0.45684 & 0.03286 \\ 0 & 0 & 0.00801 \end{bmatrix} \cdot \begin{bmatrix} X \\ Y \\ Z \end{bmatrix}$$

to convert from CIE 1931 Standard Observer color matching functions to the LMS cone response color space.

The stimuli were created for seven color directions: black to white, green to red, yellow to blue, pink to green-cyan, green to light-pink, dark-red to cyan, and green-yellow to blue-violet (see Tab. 1 and Fig. 1). We used the color axes that generate achromatic (C1), chromatic (C2,C3), and mixed chromatic/achromatic stimuli (M4-M7). As our measurements are motivated by the future computer graphics applications, we used the starting and ending points

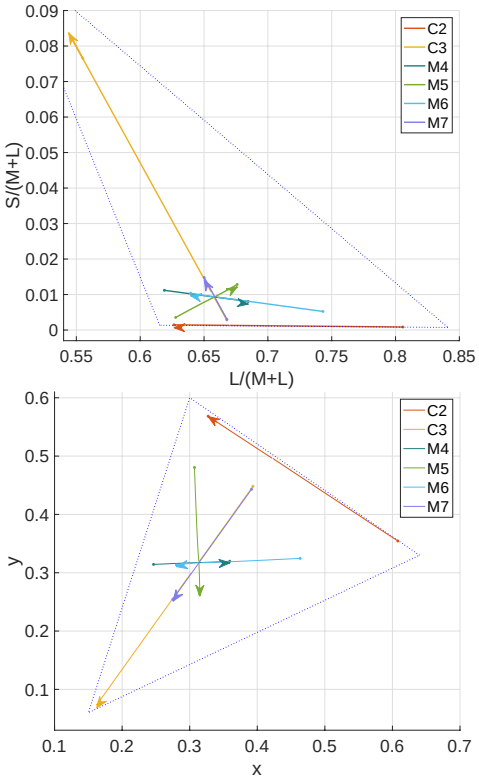

Figure 1: The color directions for chromatic and mixed chromatic/achromatic stimuli from Tab. 1 plotted in the Boynton-MacLeod diagram (top) and CIE 1931 xy chromaticity space (bottom). The outside dotted lines depict the monitor gamut. The actual color directions are indicated by the arrow markers. Note that luminance component of M4-M7 is skipped.

of the mixed color axes characteristic for the RGB color space (see details in the last column of Tab. 1).

The whole stimulus covered 8° of visual field. However, it was attenuated by Gaussian envelope with $\sigma = 70$ and maximum contrast level was displayed only in the center of the stimulus.

To make sure that our display shows accurate stimuli, we measured the Yxy color values for the whole range of contrast parameter c for each color direction. These measurements were captured using the Specbos 1211 spectro-radiometer and additionally confirmed using the Minolta CS100A chroma meter. The results of the measurements were fitted to the polynomials and used to approximate the cone contrast (C_c) based on the stimulus contrast parameter (c) and color direction.

3.2 Procedure

During the experiment the stimulus was observed from a fixed distance of $90cm$, which gave an angular resolution of 60 pixels per visual degree (a chin rest was used). Participants were asked to directly look at the green cross displayed on the right side of the display and do not move their eyes (see Fig. 3). The display was

Table 1: The Yxy values and LMS cone excitations of the end-points (From color and To color) of the color directions. ΔY **denotes difference in luminance between end-points.** $ch_b(C2) = [0.2080, -0.6772, 0]$**,** $ch_b(C3) = [-0.2080, -0.6772, 0.0797]$**.**

	Color direction	From color						To color							
		Y	x	y	L	M	S	Y	x	y	L	M	S	ΔY	ch_{rgb}
C1	black to white	9.62	0.31	0.32	6.33	3.29	0.09	85.06	0.31	0.32	55.97	29.09	0.80	75.45	[1,1,1]
C2	green to red	20.55	0.61	0.35	16.56	3.99	0.02	20.10	0.33	0.57	12.59	7.51	0.03	0.45	$ch_b(C2)$
C3	yellow to blue	6.91	0.39	0.45	4.62	2.30	0.02	6.65	0.17	0.08	3.69	2.96	0.51	0.26	$ch_b(C3)$
M4	pink to green-cyan	39.60	0.25	0.31	24.51	15.09	0.44	56.51	0.36	0.32	38.69	17.83	0.45	16.91	[1,0,0]
M5	green to light-pink	36.64	0.31	0.48	23.00	13.64	0.13	59.21	0.31	0.26	40.02	19.19	0.76	22.57	[1,0,1]
M6	dark-red to cyan	18.24	0.46	0.32	13.56	4.69	0.10	77.23	0.28	0.31	49.38	27.85	0.80	58.99	[0,1,1]
M7	green-yellow to blue-violet	45.17	0.39	0.44	30.17	15.00	0.13	51.48	0.28	0.25	33.46	18.01	0.76	6.31	[0,0,1]

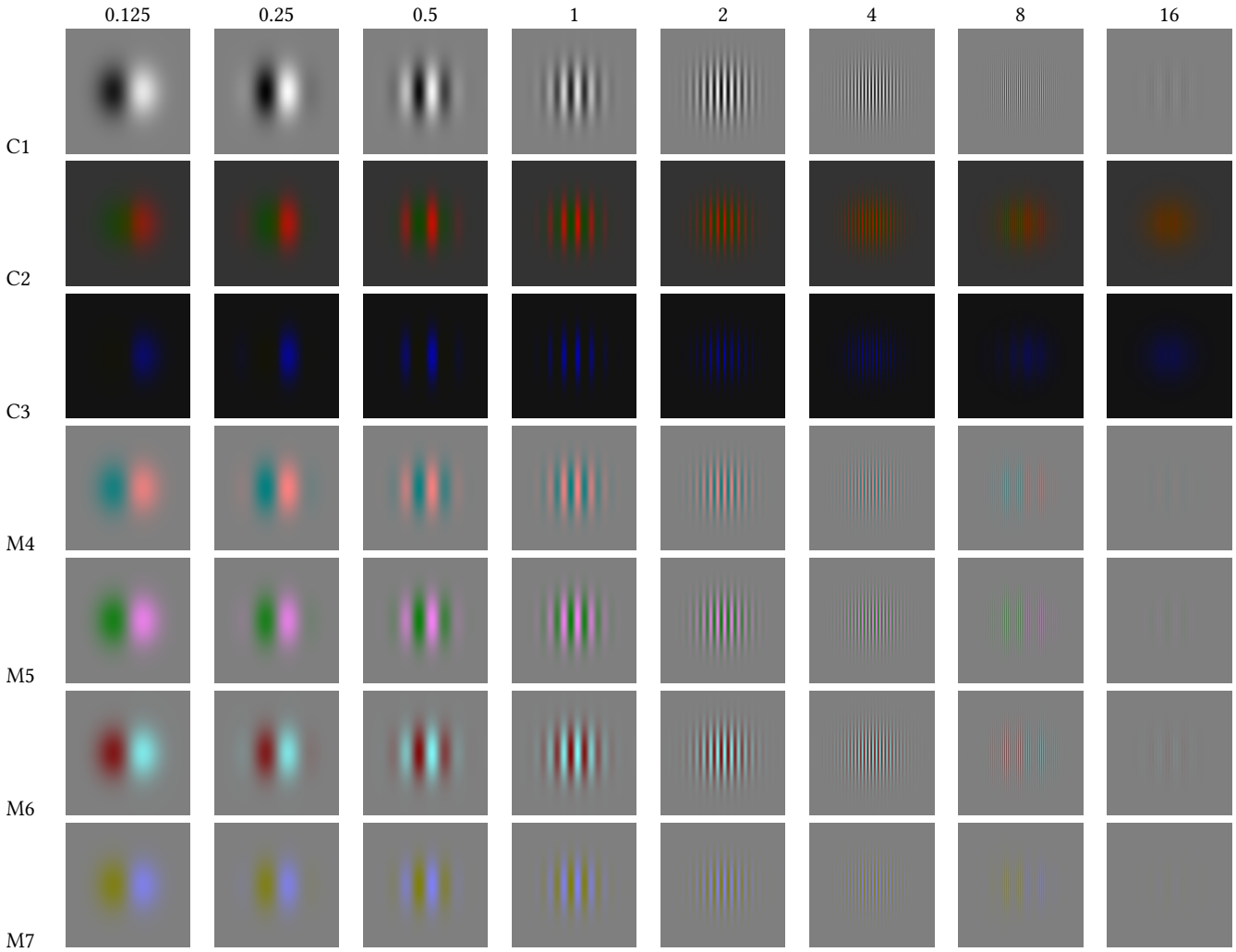

Figure 2: Examples of achromatic (C1), chromatic (C2-C3), and mixed achromatic and chromatic (M4-M7) stimuli. Frequencies of the stimuli are expressed in cycles-per-degree).

moved to the left so that observers look straight at its right part. The sine-grating stimulus was displayed in random orientation (horizontal or vertical) on the left side of the screen at the arbitrary eccentricity measured from the green cross. A task was to recognize the horizontal or vertical direction of the sine-grating by pressing the *up* or *right* keyboard keys.

To find the threshold magnitude of the sine-grating, we used the QUEST adaptive procedure [Watson and Pelli 1983]. The QUEST procedure takes into account the distribution of responses near the threshold and the actual shape of the psychometric function [Mantiuk et al. 2012]. Many trials are repeated while varying the magnitude of the stimulus. The magnitude of the next trial is determined on the basis of the observer's responses in previous trials. In our experiment, a threshold magnitude of visible contrast was searched using the log10(c) units. QUEST adaptively determines the degree of contrast for the next trial based on the observer's correct or incorrect response for the current trial. We used the QUEST implementation from Psychtoolbox (version 3). The maximum number of trials was set to 50. The procedure was repeated for eccentricities of 5°, 10°, 15°, 20°, and 27°. We also measured the contrast threshold at the fovea (i.e. for eccentricity of 0°).

Following methodology presented in [Chwesiuk and Mantiuk 2017], we use an eye tracker to prevent registration of the results after the unintended movement of the eyes towards the stimulus. This eye movement can result in the registration of the foveal contrast sensitivity rather than peripheral contrast sensitivity and should be strictly controlled in the case of the experiments investigating peripheral vision. To test if the eye tracker-based experiment gives the results consistent with the flickering technique (displaying the stimulus for a short time [Peli et al. 1991]), we performed a pilot experiment without eye tracker. Both techniques revealed comparable accuracy.

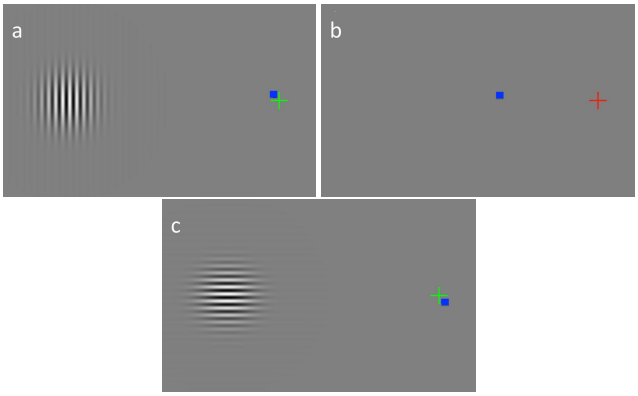

Figure 3: Using the eye tracking to ensure the correct gaze direction. The green/red cross depicts the required gaze direction. The blue point simulates the gaze location captured by eye tracker. If the distance between gaze location and the cross exceeds the accuracy of the eye tracker, the stimulus is hidden, and redrawn with random orientation.

3.3 Apparatus and display calibration

The experiments were run using Sony PVM-A250 TRIMASTER EL, 1920x1080 pixel resolution display. It offers good luminance reproduction with a 10-bit OLED panel. The 10-bit depth resolution was required in our near-threshold detection experiment to reliable display stimuli of very low contrasts. We set the display color profile to sRGB. The correctness of the display calibration was confirmed using the Minolta CS-100A chroma meter.

The EyeTribe 60Hz eye tracker was used to control the observers' gaze location and prevent unintended eye movements toward the stimulus. The EyeTribe works with sufficient accuracy and frequency to detect eye movement and hide the stimulus. Making an erroneous measurement would require a conscious look at the stimulus and return the eye to the original position within 17 milliseconds of the eye tracker latency [Chwesiuk and Mantiuk 2016].

3.4 Participants

We asked 5 volunteer observers to conduct the experiment (age between 21 and 47 years, average age 27.67, one female, four males). Observers declared normal or corrected to normal vision and correct color vision. Before the experiment, we briefly described to each participant the motivation behind the detection threshold measurement but not the details of our strategy. The experiment was divided into many sessions, in each of them, the thresholds were tested for only one frequency of the stimulus but for all eccentricities. The average observer finished a session in approximately 10 minutes. All sessions were performed within 5-8 weeks at different intervals depending on the fatigue reported by the participant.

4 RESULTS

In this Section we present results of the measurements for achromatic CSF at fovea for frequencies of 0.125, 0.25, 1, 4, 8, 16*cpd*, for achromatic CSF for the same range of frequencies but at eccentricities of 5°, 10°, 15°, 20°, 27°, and for six color directions for the same eccentricities but only for frequency of 2*cpd*.

4.1 Contrast sensitivity function for achromatic stimuli

To verify that our experimental setup generates the results consistent with the previous work, we measured the contrast sensitivity function for the foveal vision. Fig. 4 compares our results with Barten's CSF model [Barten 1999] and the measurements from [Kim et al. 2013]. The CSF averaged over all observers shows a typical band-pass characteristic. As can be seen in Fig. 4, the CSF values are lower than those measured by Kim et al. The discrepancies can be explained by the different size of the stimuli in both experiments. To prove this observation we performed a pilot study using twice the size of the stimulus used in the main experiment. The results are presented as a green line in Fig. 4, which is closer to the contrast sensitivity measured in Kim et al. For further measurements, we kept the same size of the stimulus because a larger size could give erroneous measurements for a peripheral vision where the angular separation of the stimulus is important.

We achieved the peak contrast sensitivity for a frequency of 4*cpd*. However, Barten's CSF model shows the peak sensitivity for 2*cpd*. Also, Kim et al. data are shifted towards 2*cpd*. Therefore, in the measurement for the peripheral vision, we decided to use the stimuli of 2*cpd*.

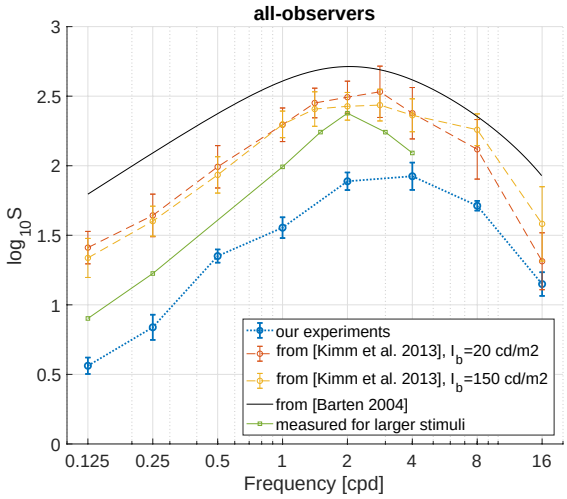

Figure 4: Measurements of the achromatic contrast sensitivity function (C1) averaged over all observers, and the CSFs from other studies. The error-bars denote the standard error of mean.

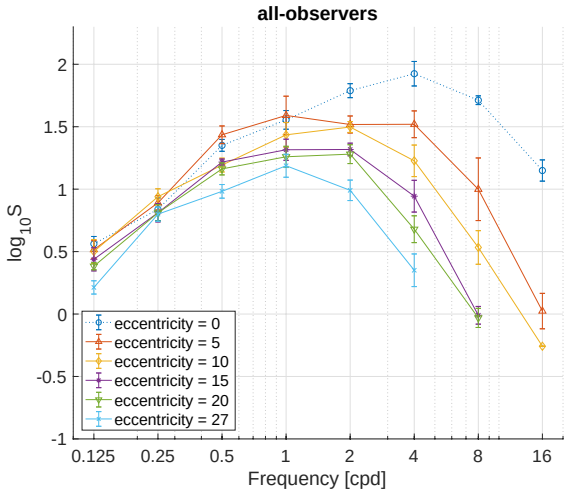

Figure 5: Measurements of the achromatic gaze-dependent CSF (C1) averaged over all observers. Different line colors denote different eccentricities. The error-bars denote the standard error of mean. The dotted line shows CSF for the foveal vision.

4.2 Contrast sensitivity function for achromatic stimuli and peripheral vision

We measured the contrast sensitivity for achromatic stimuli (black to white) for eccentricities varying from 5° to 27°. The results averaged over all observers are presented in Fig. 5. For the frequencies of 0.125*cpd* and 0.25*cpd*, the contrast sensitivity is close to the sensitivity measured at fovea but for higher frequencies, the sensitivity begins to decrease. This decrease is higher for higher frequencies. For 8*cpd* difference in contrast sensitivity between fovea and eccentricity of 20° is close to 2 orders of magnitude. Threshold values for frequency of 8*cpd* and eccentricity of 27° as well as the frequency of 16*cpd* and eccentricity of 20° and 27° were not measured because observers were not able to identify the orientation of the stimuli even for the maximum contrast value available on our display.

The results for individual observers are presented in Fig. 6. The plots show that the measurements are relatively consistent across observers. However, irregularities in the curve shapes exist, especially for larger eccentricities. As it was mentioned before it was difficult for observers to find threshold contrast for the borderline cases of 8 and 16*cpd* and eccentricity of 20° and 27°. In some cases, the sensitivity for different eccentricities oscillates with respect to each other. We argue that these shifts are caused by measurement errors. The most consistent results were achieved for observer *mch* who completed many measurements and was relatively experienced. Despite these irregularities measured for individual observers, the curves averaged over observers consistently show that the contrast sensitivity is lower for larger eccentricities.

4.3 Contrast sensitivity function for chromatic and mixed chromatic/achromatic stimuli and peripheral vision

Fig. 7 presents measurements of the contrast sensitivity for six different color directions drawn on separate plots. All measurements were made for frequency of 2*cpd* and eccentricities from 5° to 27°. The experimental conditions were the same as for achromatic stimuli.

As can be seen in Fig. 7, the plots for all color directions show the drop of sensitivity with increasing eccentricity, also reported in other studies. This drop is comparable for all color direction and similar to the line of achromatic stimuli.

The plot for C2 shows higher sensitivity in comparison to achromatic stimulus. At the fovea, the contrast sensitivity is close to 2.6 log units, which is comparable to a value of 2.4 log units reported in [Kim et al. 2013] (see Fig. 4 in this paper). The C3 color direction is less sensitive to contrast than C2 and achromatic stimuli.

Mixed chromatic/achromatic M7 color direction has low contrast sensitivity. It can be explained by weak achromatic component in M7 ($\Delta Y = 6.31$) and the fact that M7 coincides with the part of C3 direction of the low sensitivity (see Fig. 1). Another coinciding directions, M4 and M6, show significantly different sensitivity because the sensitivity for M6 is reduced by the strong achromatic component ($\Delta Y = 58.99$).

The mixed color directions that are closer to the chromatic C2 direction show higher sensitivity (e.g. M4), especially if the achromatic component is weak. In turn, direction closer to chromatic C3 show lower sensitivity to contrast (e.g. M7). Strong achromatic component approaches contrast sensitivity to the achromatic CSF.

Fig. 8 shows the results for individual observers. The measurements are rather noisy with frequent inversion of contrasts for individual color directions. However, a decrease of the contrast sensitivity with eccentricity is clearly visible.

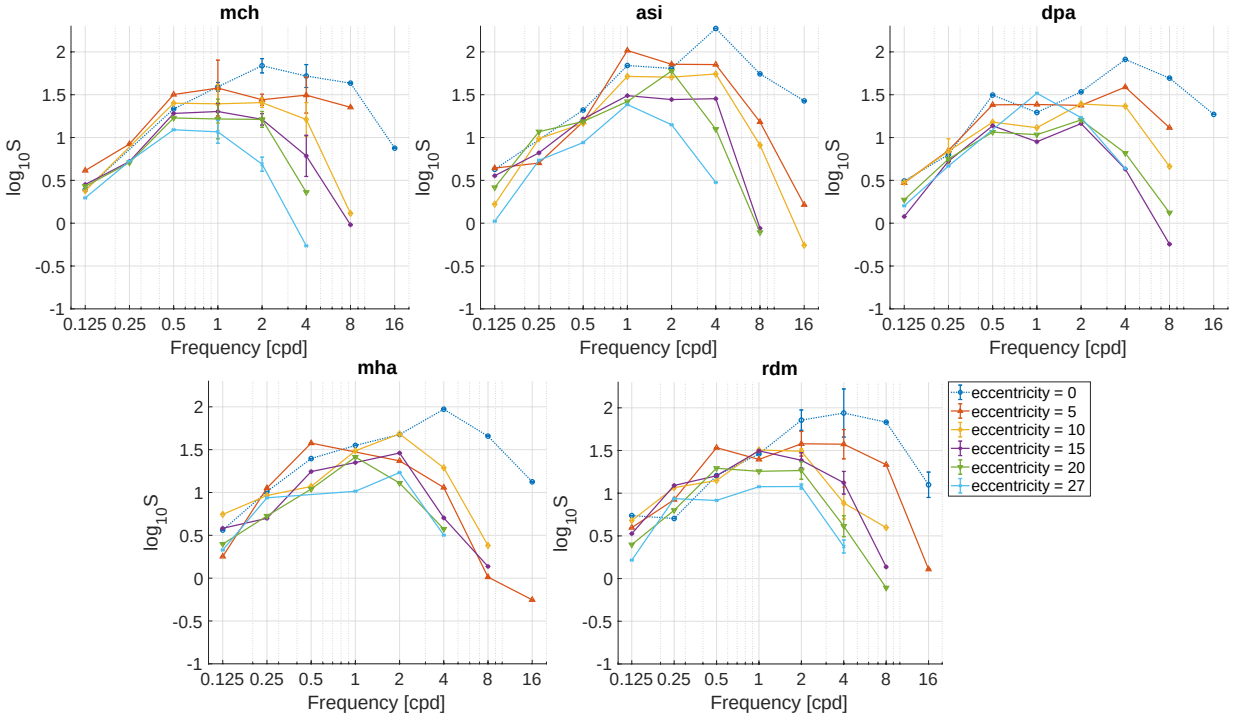

Figure 6: Measurements of the achromatic CSF (black to white) for individual observers (marked as mch, asi, dpa mha, and rdm). The annotations are the same as in Fig. 5

5 CONCLUSIONS

New contrast sensitivity measurements were conducted to capture the effect of eccentricity on contrast detection for achromatic, chromatic and mixed chromatic/achromatic stimuli. The goal was to capture color directions corresponding to the RGB color primaries used in the computer graphics applications. We believe that new data will help to predict the visibility of contrast in the image rendering systems. For example, the high resolution images are required for the VR headsets equipped with the wide field of view 4k displays. However, images with spatially varying resolution can be rendered for these devices because the observer looks only at the section of the image in the moment. This technique, called a foveated rendering, generates more samples for the central vision, while the number of samples in the periphery is significantly reduced [Siekawa et al. 2019]. The state-of-the-art techniques of the foveated rendering reduce the sampling density based on the achromatic contrast sensitivity [Tursun et al. 2019]. The inclusion of color sensitivity would allow further reduction of the number of samples because HVS is less sensitive to selected colors than to luminance contrast. As the rendering systems are based on the RGB color space, we assume that color axis associated with this space would be more suitable to model relation between colors in the image and chromatic contrast sensitivity.

We found significant differences when our data was compared to popular CSF models. We observe lower sensitivity for achromatic stimuli, which can be explained by the smaller angular size of the used stimuli. We argue that further studies on the effect of stimulus size on the contrast threshold for different color directions in the peripheral vision are needed [Nagy and Doyal 1993]. Our measurements clearly show the relation between chromatic and achromatic components in the mixed color directions. The contrast sensitivity is higher for the green-red axis and lower for the yellow-blue axis. The higher share of the achromatic component shifts the sensitivity towards the achromatic axis.

In future work, we wish to fit an analytical model that could be used to interpolate our data. Such a model was derived for foveal vision [Denes et al. 2019] but a more general model that could explain the sensitivity to contrast for the whole visual field is needed.

ACKNOWLEDGMENTS

The project was funded by the Polish National Science Centre (decision number DEC-2013/09/B/ST6/02270).

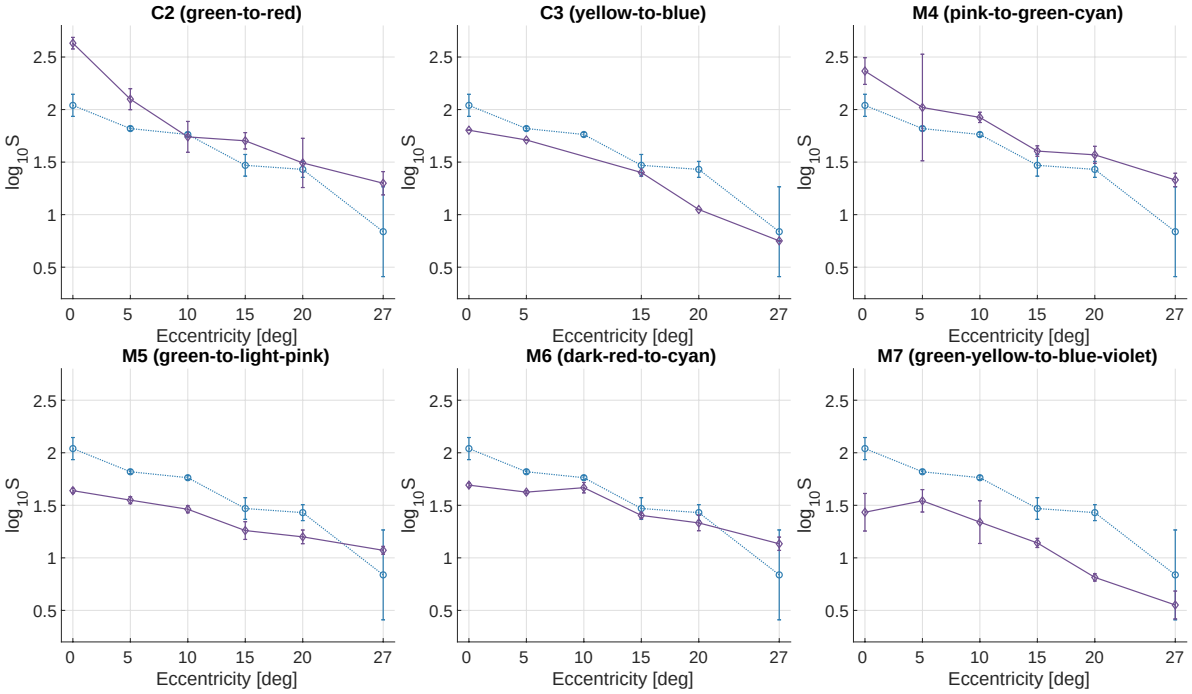

Figure 7: Measurements of the contrast sensitivity for chromatic (C2,C3) and mixed chromatic/achromatic (M4-M7) stimuli of 2*cpd* frequency averaged over all observers. The blue dotted lines show the contrast sensitivity for achromatic stimuli. The error-bars denote the standard error of mean.

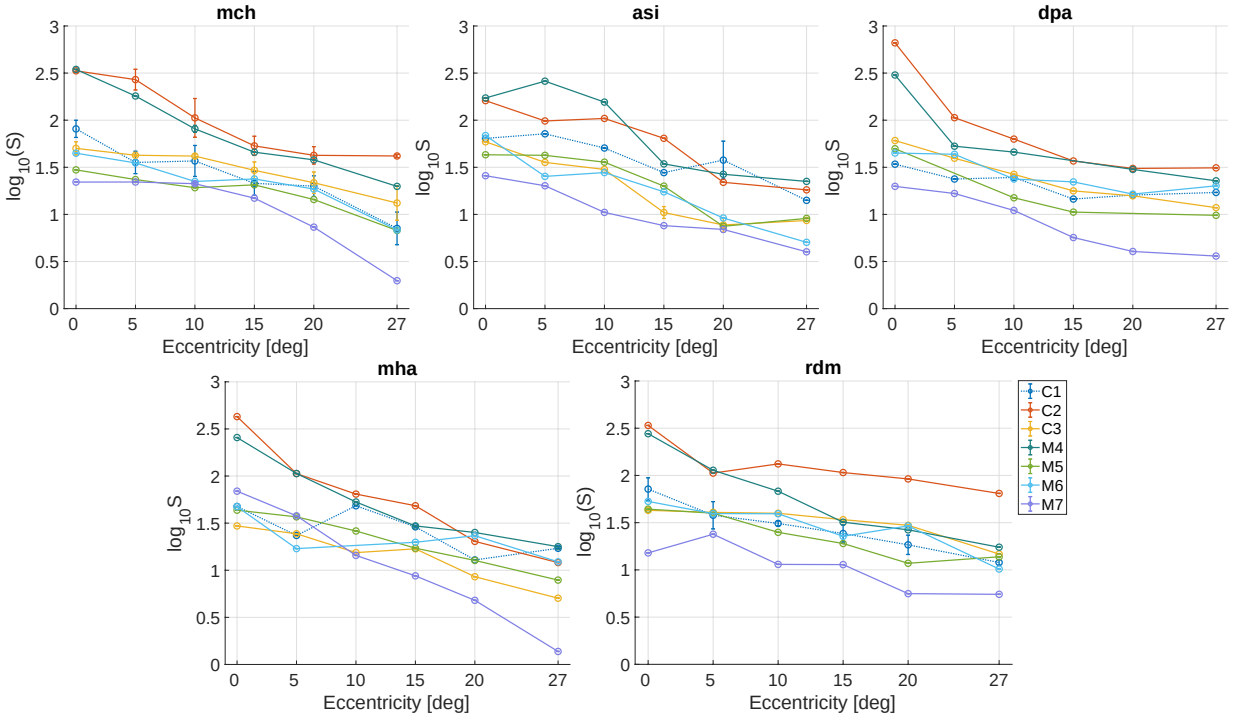

Figure 8: Measurements of the contrast sensitivity for chromatic (C2,C3) and mixed (M4-M7) color directions for individual observers and stimuli frequency of 2*cpd*. The blue dotted line shows the contrast sensitivity for achromatic stimuli.

REFERENCES

Stephen J Anderson, Kathy T Mullen, and Robert F Hess. 1991. Human peripheral spatial resolution for achromatic and chromatic stimuli: limits imposed by optical and retinal factors. *The Journal of Physiology* 442, 1 (1991), 47–64.

Martin S Banks, Allison B Sekuler, and Stephen J Anderson. 1991. Peripheral spatial vision: Limits imposed by optics, photoreceptors, and receptor pooling. *JOSA A* 8, 11 (1991), 1775–1787.

Peter GJ Barten. 1999. *Contrast sensitivity of the human eye and its effects on image quality*. Vol. 21. Spie optical engineering press Bellingham, WA.

Robert M Boynton and Naotake Kambe. 1980. Chromatic difference steps of moderate size measured along theoretically critical axes. *Color Research & Application* 5, 1 (1980), 13–23.

David H Brainard. 1997. The psychophysics toolbox. *Spatial vision* 10 (1997), 433–436.

Mark W Cannon. 1985. Perceived contrast in the fovea and periphery. *JOSA A* 2, 10 (1985), 1760–1768.

Michał Chwesiuk and Radosław Mantiuk. 2016. Acceptable System Latency for Gaze-Dependent Level of Detail Rendering. In *EG 2016 - Posters*, Luis Gonzaga Magalhaes and Rafal Mantiuk (Eds.). The Eurographics Association. https://doi.org/10.2312/egp.20161043

Michał Chwesiuk and Radosław Mantiuk. 2017. Measurements of contrast detection thresholds for peripheral vision using non-flashing stimuli. In *International Conference on Intelligent Decision Technologies*. Springer, 258–267.

Gyorgy Denes, George Ash, and RafaÅĆ K. Mantiuk. 2019. Towards a spatio-chromatic standard observer for detection. In *Human Vision and Electronic Imaging*. International Society for Optics and Photonics.

MA Díez-Ajenjo, P Capilla, and MJ Luque. 2011. Red-green vs. blue-yellow spatio-temporal contrast sensitivity across the visual field. *Journal of Modern Optics* 58, 19-20 (2011), 1736–1748.

James Gordon and Israel Abramov. 1977. Color vision in the peripheral retina II Hue and saturation. *Journal of the Optical Society of America* 67 (03 1977), 202–7. https://doi.org/10.1364/JOSA.67.000202

Thorsten Hansen, Lars Pracejus, and Karl R Gegenfurtner. 2009. Color perception in the intermediate periphery of the visual field. *Journal of Vision* 9, 4 (2009), 26–26.

R Hilz and CR Cavonius. 1974. Functional organization of the peripheral retina: Sensitivity to periodic stimuli. *Vision Research* 14, 12 (1974), 1333–1337.

Kil Joong Kim, Rafal Mantiuk, and Kyoung Ho Lee. 2013. Measurements of achromatic and chromatic contrast sensitivity functions for an extended range of adaptation luminance. In *IS&T/SPIE Electronic Imaging*. International Society for Optics and Photonics, 86511A–86511A.

Rafal Mantiuk, Anna M. Tomaszewska, and Radoslaw Mantiuk. 2012. Comparison of Four Subjective Methods for Image Quality Assessment. *Comput. Graph. Forum* 31, 8 (2012), 2478–2491.

Kathy Mullen. 1985. The contrast sensitivity of human color vision to red-green and blue-yellow chromatic gratings. *The Journal of physiology* 359 (03 1985), 381–400. https://doi.org/10.1113/jphysiol.1985.sp015591

KT Mullen. 1991. Colour vision as a post-receptoral specialization of the central visual field. *Vision research* 31, 1 (1991), 119–130.

Kathy T Mullen and Frederick A.A. Kingdom. 2002. Differential distributions of red–green and blue–yellow cone opponency across the visual field. *Visual neuroscience* 19, 1 (2002), 109–118.

Kathy T Mullen, Masato Sakurai, and William Chu. 2005. Does L/M cone opponency disappear in human periphery? *Perception* 34, 8 (2005), 951–959.

Allen L Nagy and Jeffrey A Doyal. 1993. Red-green color discrimination as a function of stimulus field size in peripheral vision. *JOSA A* 10, 6 (1993), 1147–1156.

Allen L Nagy and Steven Wolf. 1993. Red-green color discrimination in peripheral vision. *Vision research* 33, 2 (1993), 235–242.

Jessica R Newton and Rhea T Eskew. 2003. Chromatic detection and discrimination in the periphery: A postreceptoral loss of color sensitivity. *Visual neuroscience* 20, 5 (2003), 511–521.

Cornelis Noorlander, Jan J. Koenderink, R J den Ouden, and B Wigbold Edens. 1983. Sensitivity to spatio-temporal color contrast in the peripheral visual field. *Vision research* 23 (02 1983), 1–11. https://doi.org/10.1016/0042-6989(83)90035-4

Eli Peli, Jian Yang, and Robert B Goldstein. 1991. Image invariance with changes in size: The role of peripheral contrast thresholds. *JOSA A* 8, 11 (1991), 1762–1774.

Denis G Pelli and Peter Bex. 2013. Measuring contrast sensitivity. *Vision research* 90 (2013), 10–14.

JS Pointer and RF Hess. 1989. The contrast sensitivity gradient across the human visual field: With emphasis on the low spatial frequency range. *Vision research* 29, 9 (1989), 1133–1151.

JG Robson and Norma Graham. 1981. Probability summation and regional variation in contrast sensitivity across the visual field. *Vision research* 21, 3 (1981), 409–418.

Adam Siekawa, Michał Chwesiuk, Radosław Mantiuk, and Rafał Piórkowski. 2019. Foveated Ray Tracing for VR Headsets. In *MultiMedia Modeling*, Ioannis Kompatsiaris, Benoit Huet, Vasileios Mezaris, Cathal Gurrin, Wen-Huang Cheng, and Stefanos Vrochidis (Eds.). Springer International Publishing, Cham, 106–117.

James P Thomas. 1987. Effect of eccentricity on the relationship between detection and identification. *JOSA A* 4, 8 (1987), 1599–1605.

Okan Tarhan Tursun, Elena Arabadzhiyska, Marek Wernikowski, Radosław Mantiuk, Hans-Peter Seidel, Karol Myszkowski, and Piotr Didyk. 2019. Luminance-Contrast-Aware Foveated Rendering. *ACM Transactions on Graphics (Proc. of SIGGRAPH19)* (2019).

John E Vanston and Michael A Crognale. 2018. Effects of eccentricity on color contrast. *JOSA A* 35, 4 (2018), B122–B129.

Andrew B Watson. 2000. Visual detection of spatial contrast patterns: Evaluation of five simple models. *Optics Express* 6, 1 (2000), 12–33.

Andrew B Watson and Denis G Pelli. 1983. QUEST: A Bayesian adaptive psychometric method. *Perception & psychophysics* 33, 2 (1983), 113–120.

Sophie M Wuerger, Andrew B Watson, and Albert J Ahumada. 2002. Towards a spatio-chromatic standard observer for detection. In *Human Vision and Electronic Imaging VII*, Vol. 4662. International Society for Optics and Photonics, 159–173.